

# Inner-Shell Effects on Heterogeneous Electron-Transfer Rates of Bis(1,4,7-triazacyclononane) (tacn) Redox Couples, $M(\text{tacn})_2^{3+/2+}$ ( $M = \text{Fe, Co, Ni, Ru}$ )

Philip W. Crawford\*<sup>†</sup> and Franklin A. Schultz\*<sup>‡</sup>

Departments of Chemistry, Southeast Missouri State University, Cape Girardeau, Missouri 63701-4799, and Indiana University—Purdue University at Indianapolis, 402 North Blackford Street, Indianapolis, Indiana 46202-3274

Received February 23, 1994<sup>⊗</sup>

Heterogeneous electron-transfer rates and activation parameters are reported for  $M(\text{tacn})_2^{3+/2+}$  ( $M = \text{Fe, Co, Ni, Ru}$ ; tacn = 1,4,7-triazacyclononane) complexes in aqueous sodium fluoride solution. The  $M(\text{tacn})_2^{3+/2+}$  couples are chemically reversible, outer-sphere, one-electron transfers whose redox-induced changes in metal–nitrogen bond distance range from 1 to 18 pm depending on the identity of  $M$ . Double-layer corrected standard heterogeneous rate constants decrease in a sequence ( $\text{Ru} \approx \text{Fe} > \text{Ni} \gg \text{Co}$ ) that is qualitatively in accord with this structural feature. Inner-shell contributions to the electrochemical activation process are obtained from temperature-dependent measurement of the standard heterogeneous rate constants and subtraction of an outer-shell contribution of  $15 \text{ kJ mol}^{-1}$  calculated by the mean spherical approximation. Values of  $\Delta H_{\text{is}}^\ddagger$  are 1, 7–12, 8, and  $55 \text{ kJ mol}^{-1}$  are determined for Ru, Fe, Ni, and Co, respectively, in contrast to values of 0, 1, 9, and  $25 \text{ kJ mol}^{-1}$  calculated from a simple harmonic oscillator expression for  $M\text{—N}$  bond stretching. The  $M(\text{tacn})_2^{3+/2+}$  couples exhibit half-reaction entropies ( $\Delta S_{\text{rc}}^\circ$ ) and entropies of activation ( $\Delta S^\ddagger$ ) which correlate with the experimental inner-shell barriers. The origin of the entropic terms, the discrepancies in  $\Delta H_{\text{is}}^\ddagger$  values, and the metal dependence of these quantities are attributed to differences in vibrational partition functions between products and reactants (Richardson, D. E.; Sharpe, P. *Inorg. Chem.* **1991**, *30*, 1412) which become significant when inner-shell frequencies are low and change significantly upon redox.

## Introduction

A current focus in electron-transfer chemistry is quantitative examination of the correlation between molecular structure and reactivity predicted by Marcus–Hush theory.<sup>1–3</sup> One expectation of this theory is that the rates of homogeneous and heterogeneous electron-transfer reactions will be slow and thus exhibit a significant dependence on structure when large changes in nuclear coordinates accompany a change in oxidation state. Systems with small inner-shell barriers, wherein the kinetics are dominated by the outer-shell (solvent) reorganization energy, have been studied extensively.<sup>4</sup> However, few investigations have focused on reactions characterized by a large inner-shell barrier.<sup>5,6</sup> One reason for this may be that the number of redox

couples having significant inner-shell barriers which can be altered in a systematic fashion is small.

A series of molecules that meets this requirement are the bis-(1,4,7-triazacyclononane) (tacn)  $M(\text{III})$  and  $M(\text{II})$  complexes<sup>7</sup> with  $M = \text{Fe, Co, Ni, and Ru}$ . The two tacn ligands are fully coordinated to both oxidation states of these metals, which ensures that the following one-electron transfer is chemically reversible and occurs by an outer-sphere mechanism:



Because the size, stoichiometry, and charge of the complexes are the same, outer-shell contributions to the dynamics of reaction 1 should be equal. Thus, inner-shell effects on electron-transfer rates can be investigated systematically. The Fe, Co, Ni, and Ru members of the series are selected for study because (i) reduction of these compounds is accompanied by varying degrees of metal–ligand bond lengthening depending on the identity of  $M$ , (ii) structural data for estimation of inner-shell barrier heights are available for both oxidation states of these metals,<sup>8–13</sup> and (iii) rate constants of homogeneous electron self-exchange have been measured directly or deduced from redox

<sup>†</sup> Southeast Missouri State University.

<sup>‡</sup> Indiana University—Purdue University at Indianapolis.

<sup>⊗</sup> Abstract published in *Advance ACS Abstracts*, July 15, 1994.

- (1) (a) Marcus, R. A. *J. Chem. Phys.* **1956**, *24*, 966. (b) Marcus, R. A. *J. Chem. Phys.* **1965**, *43*, 679. (c) Marcus, R. A. *Electrochim. Acta* **1968**, *13*, 995. (d) Marcus, R. A. *Angew. Chem., Int. Ed. Engl.* **1993**, *32*, 1111.
- (2) (a) Hush, N. S. *Trans. Faraday Soc.* **1961**, *57*, 557. (b) Hush, N. S. *Prog. Inorg. Chem.* **1967**, *8*, 391. (c) Hush, N. S. *Electrochim. Acta* **1968**, *13*, 1005.
- (3) (a) Reynolds, W. L.; Lumry, R. W. *Mechanisms of Electron Transfer*; Ronald Press: New York, 1966. (b) Ulstrup, J. *Charge Transfer Processes in Condensed Media*; Springer-Verlag: Berlin, 1979. (c) Cannon, R. D. *Electron Transfer Reactions*; Butterworths: London, 1980. (d) Sutin, N. *Prog. Inorg. Chem.* **1983**, *30*, 441.
- (4) For recent review of this subject see: (a) Weaver, M. J. *Chem. Rev.* **1992**, *92*, 463. (b) Heitele, H. *Angew. Chem., Int. Ed. Engl.* **1993**, *32*, 359. (c) Fawcett, W. R.; Opallo, M. *Angew. Chem., Int. Ed. Engl.* **1994**, *33*, 0000.
- (5) Investigations of homogeneous self-exchange reactions having large inner-shell barriers include: (a) Brunschwig, B. S.; Creutz, C.; Macartney, D.; Sham, T.-K.; Sutin, N. *Faraday Discuss. Chem. Soc.* **1982**, *74*, 113. (b) Stanbury, D. M.; Lednický, L. A. *J. Am. Chem. Soc.* **1984**, *106*, 2847. (c) Nelsen, S. F.; Blackstock, S. C.; Kim, Y. J. *Am. Chem. Soc.* **1987**, *109*, 677.

- (6) Heterogeneous investigations with this characteristic include: (a) Feng, D.; Schultz, F. A. *Inorg. Chem.* **1988**, *27*, 2144. (b) Nielson, R. M.; Weaver, M. J. *J. Electroanal. Chem.* **1989**, *260*, 15. (c) Phelps, D. K.; Ram, M. T.; Wang, Y.; Nelsen, S. F.; Weaver, M. J. *J. Phys. Chem.* **1993**, *97*, 181.
- (7) Chaudhuri, P.; Wieghardt, K. *Prog. Inorg. Chem.* **1987**, *35*, 329.
- (8) Bernhard, P.; Bürgi, H. B.; Raselli, A.; Sargeson, A. M. *Inorg. Chem.* **1989**, *28*, 3234.
- (9) Boeyens, J. C. A.; Forbes, A. G. S.; Hancock, R. D.; Wieghardt, K. *Inorg. Chem.* **1985**, *24*, 2926.
- (10) Wieghardt, K.; Walz, W.; Nuber, B.; Weiss, J.; Ozarowski, A.; Stratemeier, H.; Reinen, D. *Inorg. Chem.* **1986**, *25*, 1650.
- (11) Zompa, L. J.; Margulis, T. N. *Inorg. Chim. Acta* **1978**, *28*, L157.
- (12) Mikami, W.; Kuroda, R.; Konno, M.; Saito, Y. *Acta Crystallogr.* **1977**, *B33*, 1485.

**Table 1.** Structural Data, Calculated Inner-Shell Activation Enthalpies, and Homogeneous Electron Self-Exchange Rates for M(tacn)<sub>2</sub><sup>3+/2+</sup> Couples

M	config	M <sup>III</sup> —N (pm)	M <sup>II</sup> —N (pm)	Δa (pm)	(ΔH <sup>‡</sup> <sub>is</sub> ) <sub>calc</sub> <sup>a</sup> (kJ mol <sup>-1</sup> )	k <sub>ex</sub> <sup>b</sup> (M <sup>-1</sup> s <sup>-1</sup> )
Ru	(t <sub>2g</sub> ) <sup>5</sup> /(t <sub>2g</sub> ) <sup>6</sup>	209.7(8) <sup>c</sup>	210.5(10) <sup>c</sup>	0.8	0	5 × 10 <sup>4</sup> <sup>d</sup>
Fe	(t <sub>2g</sub> ) <sup>5</sup> /(t <sub>2g</sub> ) <sup>6</sup>	199(1) <sup>e</sup>	203(1) <sup>e</sup>	4	1	(6 × 10 <sup>3</sup> ) <sup>f</sup>
Ni	(t <sub>2g</sub> ) <sup>6</sup> (e <sub>g</sub> ) <sup>1</sup> /(t <sub>2g</sub> ) <sup>6</sup> (e <sub>g</sub> ) <sup>2</sup>	197.1(10), 210.9(5) <sup>g,h</sup>	210.5(9) <sup>i</sup>	13.4, 0.4	9 <sup>h</sup>	(1.6 × 10 <sup>3</sup> ) <sup>j</sup>
Co	(t <sub>2g</sub> ) <sup>6</sup> /(t <sub>2g</sub> ) <sup>5</sup> (e <sub>g</sub> ) <sup>2</sup>	197.4(5) <sup>k</sup>	215.5(33) <sup>i</sup>	18.1	25	1.9 × 10 <sup>-1</sup> <sup>m</sup>

<sup>a</sup> Calculated from eq 4 using a reduced force constant of  $f_i = 170 \text{ N m}^{-1}$  for all complexes. <sup>b</sup> In  $\mu = 0.1 \text{ M}$  aqueous solution at 23 or 25 °C. Values in parentheses are deduced from redox cross reactions. <sup>c</sup> Structural data for the Ru(III) and Ru(II) complexes of 3,6,10,13,16,19-hexaaza-bicyclo[6.6.6]heptane (sarcophagine = sar) and its 1-methyl derivative, respectively, from ref 8. <sup>d</sup> Reference 14. <sup>e</sup> Reference 9. <sup>f</sup> Rate constant for Fe(sar)<sup>3+/2+</sup> self-exchange.<sup>15</sup> <sup>g</sup> Reference 10. <sup>h</sup> [Ni(tacn)<sub>2</sub>]<sub>2</sub>(S<sub>2</sub>O<sub>6</sub>)<sub>3</sub> · 7H<sub>2</sub>O is Jahn–Teller distorted in the solid state<sup>10</sup> with four short and two long Ni<sup>III</sup>—N bonds; the calculated inner-shell barrier is the sum of the individual bond distortion enthalpies. <sup>i</sup> Reference 11. <sup>j</sup> Reference 16, corrected to  $\mu = 0.1 \text{ M}$ .<sup>14</sup> <sup>k</sup> Structural data for 2-methyl derivative (Metacn).<sup>12</sup> <sup>l</sup> Reference 13. <sup>m</sup> Rate constant for Co((S)-Metacn)(tacn)<sup>3+/2+</sup>/Co((R)-Metacn)(tacn)<sup>2+</sup> electron exchange.<sup>13</sup>

cross-reactions for all four examples of reaction 1 with tacn or a related macrocyclic ligand.<sup>13–16</sup> Table 1 summarizes structural and kinetic data for these compounds.

This manuscript reports measurement of heterogeneous electron-transfer rates, activation barriers, and pre-exponential factors for reaction 1 in aqueous sodium fluoride solution. Results are interpreted in terms of the Marcus–Hush theory applied to electrode reactions.<sup>1b,17</sup>

$$k_{s,h} = A e^{\Delta S^\ddagger/R} e^{-(\Delta H^\ddagger_{is} + \Delta H^\ddagger_{os})/RT} \quad (2)$$

$$A = K_p \kappa_{el} \Gamma_n \nu_n \quad (3)$$

In eqs 2 and 3  $k_{s,h}$  is the standard heterogeneous rate constant,  $\Delta H^\ddagger_{is}$  and  $\Delta H^\ddagger_{os}$  are the inner- and outer-shell enthalpies of activation,  $\Delta S^\ddagger$  is the entropy of activation, and  $A$  is the product of four terms in the encounter pre-equilibrium model of heterogeneous electron-transfer kinetics:<sup>17</sup>  $K_p$ , the equilibrium constant for formation of the precursor state to electron transfer,  $\kappa_{el}$ , the electron tunneling coefficient,  $\Gamma_n$ , the nuclear tunneling factor, and  $\nu_n$ , the nuclear frequency factor. Our objectives are, first, to ascertain if experimental barrier heights estimated from the temperature dependence of  $k_{s,h}$ <sup>18</sup> (and corrected for  $\Delta H^\ddagger_{os}$  and other enthalpic contributions to the electrochemical activation process<sup>19</sup>) compare favorably with the inner-shell enthalpies of activation calculated for reaction 1. This is done by means of eq 4, where  $\Delta a$  is the difference in metal–ligand bond

$$(\Delta H^\ddagger_{is})_{\text{calc}} = \frac{1}{2} \sum f_i (\Delta a/2)^2 \quad (4)$$

distance between the two oxidation states and  $f_i$  is the reduced force constant for metal–ligand bond stretching. Second, we wish to determine if inner-shell effects contribute in any way to the pre-exponential factor of eq 2. Because significant differences in metal–ligand bond lengthening accompany M(tacn)<sub>2</sub><sup>3+</sup> reduction, inner-shell factors, if present, should be observable for these half-reactions. The present manuscript reports the measurement and interpretation of such effects.

## Experimental Section

**Materials.** The complexes [Fe(tacn)<sub>2</sub>]<sub>2</sub>Br<sub>3</sub> · 5H<sub>2</sub>O,<sup>20</sup> [Co(tacn)<sub>2</sub>]<sub>2</sub>Br<sub>3</sub> · H<sub>2</sub>O,<sup>21</sup> and [Ni(tacn)<sub>2</sub>]<sub>2</sub>Cl<sub>2</sub> · 4H<sub>2</sub>O<sup>22</sup> were prepared by following literature preparations for the chloride salts and characterized by electronic absorption spectroscopy. The halides were converted to the corresponding hexafluorophosphates by ion-exchange chromatography on a Sephadex DEAE A-25 column. [Ru(tacn)<sub>2</sub>](PF<sub>6</sub>)<sub>2</sub>, synthesized as described in ref 23, was a generous gift from Professor Karl Wieghardt. 1,4,7-Triazacyclononane and sodium fluoride were obtained from the Aldrich Chemical Co. in the highest purity available and used as received. Solutions were prepared with deionized water.

**Methods.** Cyclic voltammetric measurements were made using a PAR 173/179 potentiostat, a Hewlett Packard 3300A function generator, and a Nicolet 4094C/4570 digitizing oscilloscope. Chronocoulometric measurements were made with a BAS-100 potentiostat. A three-electrode cell configuration was employed and consisted of a Pt or amalgamated Au disk of 50–127-μm diameter as a working electrode, a Pd wire auxiliary electrode, and a saturated calomel (SCE) reference electrode. The last was separated from the sample solution by a vycortipped salt bridge filled with NaF electrolyte of the appropriate concentration. Temperature-dependent measurements were carried out by the nonisothermal cell technique<sup>24</sup> in an FTS Multi-Cool bath with temperature controlled to ±0.2 °C.

The working electrodes were fabricated by sealing Pt or Au wire (Aldrich) of appropriate diameter into soft glass. These were polished on 3.0-μm silica paper and then successively with 1.0-, 0.3-, and 0.05-μm aqueous alumina suspensions (Buehler) on a polishing cloth. Before use, each electrode was polished with 0.05-μm alumina, washed with distilled water, sonicated for 10 min, and rinsed again with distilled water. The amalgamated electrodes were prepared by dipping a dry gold wire electrode into triply distilled mercury (Bethlehem). The electrode surfaces were examined under magnification to verify the completeness of amalgamation.

Standard heterogeneous rate constants were measured by cyclic voltammetry using the procedure of Nicholson.<sup>25</sup> Positive feedback was not employed. Rather, the guidelines of Evans et al.<sup>26</sup> were followed to ensure that measurements were undistorted by  $iR$  drop and nonplanar diffusion. The potential scan rate was limited to values for which the product of twice the voltammetric peak current times the uncompensated solution resistance was <2 mV and the contribution from nonplanar diffusion was <3%. For example, at 1 mM complex concentration in 1 M NaF at 25 °C sweep rates were kept within the range of 17 to 328 V s<sup>-1</sup> at the 50-μm radius electrode. The uncompensated solution resistance was calculated<sup>27</sup> from the cell

- (13) Küppers, H.-J.; Neves, A.; Pomp, C.; Ventur, D.; Wieghardt, K.; Nuber, B.; Weiss, J. *Inorg. Chem.* **1986**, *25*, 2400.  
 (14) Bernhard, P.; Sargeson, A. M. *Inorg. Chem.* **1988**, *27*, 2582.  
 (15) Bernhard, P.; Sargeson, A. M. *Inorg. Chem.* **1987**, *26*, 4122.  
 (16) (a) McAuley, A.; Norman, P. R.; Olubuyide, O. *Inorg. Chem.* **1984**, *23*, 1938. (b) McAuley, A.; Norman, P. R.; Olubuyide, O. *J. Chem. Soc., Dalton Trans.* **1984**, 1501.  
 (17) (a) Hupp, J. T.; Weaver, M. J. *J. Electroanal. Chem.* **1983**, *152*, 1. (b) Weaver, M. J. In *Comprehensive Chemical Kinetics*; Compton, R. G., Ed.; Elsevier: Amsterdam, 1987; Vol. 27, pp 1–60.  
 (18) (a) Weaver, M. J. *J. Phys. Chem.* **1976**, *80*, 2645. (b) Weaver, M. J. *J. Phys. Chem.* **1979**, *83*, 1748.  
 (19) Fawcett, W. R.; Kovacova, Z. *J. Electroanal. Chem.* **1990**, *292*, 2.

- (20) Wieghardt, K.; Schmidt, W.; Herrmann, W.; Küppers, H.-J. *Inorg. Chem.* **1983**, *22*, 2953.  
 (21) Koyama, H.; Yoshino, T. *Bull. Chem. Soc. Jpn.* **1972**, *45*, 481.  
 (22) Yang, R.; Zompa, L. J. *Inorg. Chem.* **1976**, *15*, 1499.  
 (23) Wieghardt, K.; Herrmann, W.; Koeppen, M.; Jibril, I.; Huttner, G. Z. *Naturforsch.* **1984**, *39b*, 1335.  
 (24) Yee, E. L.; Cave, R. J.; Guyer, K. L.; Tyma, P.; Weaver, M. J. *J. Am. Chem. Soc.* **1979**, *101*, 1131.  
 (25) Nicholson, R. S. *Anal. Chem.* **1965**, *37*, 1351.  
 (26) Bowyer, W. J.; Engelman, E. E.; Evans, D. H. *J. Electroanal. Chem.* **1989**, *262*, 67.  
 (27) Newman, J. J. *Electrochem. Soc.* **1966**, *113*, 501.

**Table 2.**  $M(\text{tacn})_2^{3+/2+}$  Formal Potentials (V) as a Function of Sodium Fluoride Concentration at 25 °C

M	$C_{\text{NaF}}(\text{M})$				$K_{\text{ip}} (\text{M}^{-1})$	$E^{\circ'}_{3+/2+} (\text{V})$
	0.20	0.50	0.75	1.00		
Ru	0.138	0.118	0.111	0.108	4.6	0.151
Fe	-0.114	-0.127	-0.136	-0.142	5.3	-0.095
Ni	0.712	0.696	0.687	0.685	3.9	0.725
Co	-0.640	-0.656	-0.665	-0.670	6.1	-0.620

geometry and the conductivity of NaF solutions<sup>28</sup> and checked by noting (but not applying) the amount of positive feedback required to induce oscillation of the potentiostat. Peak potential separations recorded at temperatures other than 298 K were corrected<sup>29</sup> to this value prior to determination of the kinetic parameter,  $k_{s,h}/D^{1/2}$ . Values of  $k_{s,h}$  were extracted from the last term using diffusion coefficients determined by chronocoulometry. All complexes afforded approximately the same value of  $D$ , and the results obtained for  $\text{Fe}(\text{tacn})_2^{3+/2+}$  reduction were used for all calculations. The diffusion coefficient of this complex was determined to be  $10.0 \times 10^{-6}$ ,  $9.0 \times 10^{-6}$ ,  $8.6 \times 10^{-6}$ , and  $8.1 \times 10^{-6}$   $\text{cm}^2 \text{ s}^{-1}$  in 0.20, 0.50, 0.75, and 1.00 M NaF, respectively. Its temperature dependence was determined in 0.75 M NaF and found to be described by the relationship  $D = 0.0598e^{-2638/T}$ . Formal potentials were determined as the average of cathodic and anodic peak potentials in cyclic voltammetry experiments.

## Results

The  $\text{Co}(\text{tacn})_2^{3+/2+}$  and  $\text{Fe}(\text{tacn})_2^{3+/2+}$  couples are examined as reductions and the  $\text{Ni}(\text{tacn})_2^{3+/2+}$  and  $\text{Ru}(\text{tacn})_2^{3+/2+}$  couples as oxidations in aqueous sodium fluoride. This electrolyte is selected because it provides accurate data<sup>30</sup> for correction of anticipated double layer effects<sup>31</sup> and exhibits little or no anion specific adsorption<sup>32</sup> which can influence electrochemical rate constant measurements. The Co couple is studied at Hg electrodes and the Fe couple at Hg and Pt electrodes, but the potentials of the Ru and Ni couples restrict their investigation to Pt surfaces. Each couple exhibits a voltammetric response characteristic of a diffusion-limited, chemically reversible reaction as indicated by a linear dependence of peak current on the square root of scan rate and a reverse-to-forward peak current ratio of unity. The only exception to this behavior is a decrease in peak current for Ru(III) re-reduction following oxidation of  $\text{Ru}(\text{tacn})_2^{2+}$  at sweep rates below  $2 \text{ V s}^{-1}$ . This reactivity has been observed previously<sup>23</sup> and attributed to oxidation of the ligand by the electrooxidized metal center. The rate of the reaction is sufficiently slow that it does not interfere with the electrode kinetic measurements made at faster sweep rates.

**Formal Potentials.** The formal potentials of the  $M(\text{tacn})_2^{3+/2+}$  couples exhibit a dependence on the concentration of NaF electrolyte as illustrated in Table 2. The shift in potential is in the direction consistent with ion-pair formation between fluoride ion and oxidized reactant. If it is assumed that only reaction 5



contributes to the shift in  $E^{\circ'}$  with  $[\text{F}^-]$ , the data may be analyzed by use of the relationship  $\exp[f(E^{\circ'}_{3+/2+} - E^{\circ'})] = 1 + K_{\text{ip}}[\text{F}^-]$ , where  $K_{\text{ip}}$  is the ion-pair formation constant,  $E^{\circ'}_{3+/2+}$  is the potential of reaction 1 in the absence of ion-pairing, and

(28) Dobos, D. *Electrochemical Data*; Elsevier: Amsterdam, 1975; p 53.

(29) Schmitz, J. E. J.; van der Linden, J. G. M. *Anal. Chem.* **1982**, *54*, 1879.

(30) (a) Grahame, D. C. *J. Am. Chem. Soc.* **1954**, *76*, 4819. (b) Russell, C. D. *J. Electroanal. Chem.* **1963**, *6*, 486. Note that addition of 39 mV is required to correct the tabulated values of potential to an SCE reference electrode.

(31) Delahay, P. *Double Layer and Electrode Kinetics*; Wiley-Interscience: New York, 1965.

(32) Weaver, M. J.; Satterberg, T. L. *J. Phys. Chem.* **1977**, *81*, 1772.

$f = F/RT$ . Table 2 lists values of  $K_{\text{ip}}$  and  $E^{\circ'}_{3+/2+}$  for each metal. A metal-ion independent value of  $5 \pm 1 \text{ M}^{-1}$  is obtained for  $K_{\text{ip}}$ , as anticipated for a purely electrostatic interaction.

**Kinetic Data at 25 °C.** Electrode kinetic data obtained at 25 °C are collected in Table 3. As anticipated for 3+/2+ couples, experimental  $k_{s,h}$  values are sensitive to electrical double layer effects.<sup>31</sup> In addition, the oxidized reactants are ion-paired. The combined influence of these effects is accounted for by use of a model,<sup>33</sup> which assumes that the free and ion-paired forms react by parallel paths with equal standard rate constants. Corrected values of  $k_{s,h}$  are obtained from apparent experimental ones by use of the following equation:

$$(k_{s,h})_{\text{corr}} = (k_{s,h})_{\text{app}} / [Qe^{-(z_1 - \alpha)f\phi_2} e^{-\alpha f(E^{\circ'} - E^{\circ'}_{3+/2+})} + (1 - Q)e^{-(z_2 - \alpha)f\phi_2} e^{-\alpha f(E^{\circ'} - E^{\circ'}_{\text{IM}})}] \quad (6)$$

where  $Q$  is the fraction of oxidized reactant present as the free ion in bulk solution,  $z_1$  and  $z_2$  are the charges of the free and ion-paired oxidants,  $\alpha$  is the transfer coefficient (assumed to be 0.5),  $\phi_2$  is the potential at the outer Helmholtz plane (OHP), and  $E^{\circ'}$ ,  $E^{\circ'}_{3+/2+}$ , and  $E^{\circ'}_{\text{IM}}$  are the formal potentials of reaction 1 under experimental conditions, in the absence of ion-pairing and in 1 M NaF, respectively. Values of  $\phi_2$  at Hg in Table 3 are obtained from Russell's tabulation of Grahame's data.<sup>30</sup> Entries at potentials positive of the potential of zero charge (pzc) are corrected for a small amount of specifically adsorbed fluoride ion using the data of Schiffrin.<sup>34,35</sup> Values of  $\phi_2$  at platinum are estimated by assuming that the pzc at this metal is 200 mV more positive than it is at Hg.<sup>36</sup> Double layer corrections are not applied to the  $\text{Ni}(\text{tacn})_2^{3+/2+}$  data (i.e., a value of  $\phi_2 = 0$  is used in eq 6), because these are obtained at large positive potentials on Pt where the value of  $\phi_2$  is uncertain. Under the experimental conditions it is assumed that the positive charge on the electrode is compensated by adsorption of oxide, hydroxide, or fluoride ions<sup>37</sup> and that variation in  $\phi_2$  is slight. The small change in rate constant with NaF concentration is consistent with this assumption. Average values of  $(k_{s,h})_{\text{corr}}$  obtained from eq 6 are reported in the last column of Table 3.

**Activation Parameters.** Thermodynamic and kinetic activation parameters of reaction 1 in 0.75 M NaF are reported in Table 4. Half-reaction entropies,  $\Delta S^{\circ}_{\text{rc}}$ , are determined from the temperature dependence of the formal potential:

$$-FE^{\circ'} = \Delta H^{\circ}_{\text{rc}} - T\Delta S^{\circ}_{\text{rc}} \quad (7)$$

The activation parameter obtained from the slope of a plot of  $\ln(k_{s,h})_{\text{app}}$  versus reciprocal temperature is the real enthalpy of activation.<sup>18</sup>

$$\Delta H^{\dagger}_{\text{real}} = -R\partial[\ln(k_{s,h})_{\text{app}}]/\partial(1/T) \quad (8)$$

The experimental pre-exponential factor  $A' = Ae^{\Delta S^{\dagger}/R}$  (eq 2) is obtained from the intercept of this plot and also listed in Table

(33) (a) Bieman, D. J.; Fawcett, W. R. *J. Electroanal. Chem.* **1972**, *34*, 27. (b) Rodgers, R. S.; Anson, F. C. *J. Electroanal. Chem.* **1973**, *42*, 381. (c) Weaver, M. J.; Anson, F. C. *J. Electroanal. Chem.* **1975**, *65*, 737. (d) Satterberg, T. L.; Weaver, M. J. *J. Phys. Chem.* **1978**, *82*, 1784.

(34) Schiffrin, D. J. *Trans. Faraday Soc.* **1971**, *67*, 3318.

(35) In this approach,  $q_{\text{F}^-}$ , the charge due to specifically adsorbed fluoride ion, is estimated as a function of  $q_{\text{m}}$ , the charge on the metal electrode, from KF isotherms at 15 °C (Figure 11 of ref 34), and a new value of  $\phi_2$  is calculated from the relationship  $\phi_2 = (1/19.5) \sinh^{-1} [(q_{\text{m}} + q_{\text{F}^-})/11.7C_{\text{NaF}}^{1/2}]$ . (a) Weaver, M. J. *J. Electroanal. Chem.* **1978**, *93*, 231. (b) Bard, A. J.; Faulkner, L. R. *Electrochemical Methods: Fundamentals and Applications*; Wiley: New York, 1980; p 507.

(36) Frumkin, A. N.; Petrii, O. A. *Electrochim. Acta* **1975**, *20*, 347.

(37) Lane, R. F.; Hubbard, A. T. *J. Phys. Chem.* **1975**, *79*, 808.

**Table 3.** Apparent and Double-Layer Corrected Standard Heterogeneous Rate Constants for M(tacn)<sub>2</sub><sup>3+/2+</sup> Couples at 25 °C

M	C <sub>NaF</sub> (M)												Av (k <sub>s,h</sub> ) <sub>corr</sub> (cm s <sup>-1</sup> )
	0.2		0.50		0.75		1.00						
	(k <sub>s,h</sub> ) <sub>app</sub> (cm s <sup>-1</sup> )	φ <sub>2</sub> (mV)	(k <sub>s,h</sub> ) <sub>corr</sub> (cm s <sup>-1</sup> )	(k <sub>s,h</sub> ) <sub>app</sub> (cm s <sup>-1</sup> )	φ <sub>2</sub> (mV)	(k <sub>s,h</sub> ) <sub>corr</sub> (cm s <sup>-1</sup> )	(k <sub>s,h</sub> ) <sub>app</sub> (cm s <sup>-1</sup> )	φ <sub>2</sub> (mV)	(k <sub>s,h</sub> ) <sub>corr</sub> (cm s <sup>-1</sup> )	(k <sub>s,h</sub> ) <sub>app</sub> (cm s <sup>-1</sup> )	φ <sub>2</sub> (mV)	(k <sub>s,h</sub> ) <sub>corr</sub> (cm s <sup>-1</sup> )	
Ru <sup>d</sup>	0.17(2)	49	7.9	0.18(3)	30	1.4	0.21(3)	26	1.1	0.38(5)	21.5	1.3	1.3(2) <sup>c</sup>
Fe <sup>a</sup>	0.28(6)	25	2.1	0.36(6)	15	1.1	0.35(4)	11.5	0.7	0.39(6)	9	0.6	0.8(3) <sup>c</sup>
Fe <sup>b</sup>	0.21(7)	50.0	5.7	0.31(4)	33.8	3.3	0.38(7)	27.7	2.3	0.48(6)	24.0	2.0	2.5(7) <sup>c</sup>
Ni <sup>d</sup>	0.16(3)		0.17	0.16(3)		0.15	0.11(4)		0.09	0.07(1)		0.06	0.12(5)
Co <sup>b</sup>	0.43(10)	-38.4	0.012	0.27(3)	-28.7	0.022	0.16(2)	-25.2	0.018	0.10(2)	-22.8	0.014	0.016(4)

<sup>a</sup> At Pt. <sup>b</sup> At Hg. <sup>c</sup> Result in 0.2 M NaF omitted from average.

**Table 4.** Thermodynamic and Kinetic Activation Parameters for M(tacn)<sub>2</sub><sup>3+/2+</sup> Couples in 0.75 M Sodium Fluoride

M	ΔS <sup>o</sup> <sub>rc</sub> (J mol <sup>-1</sup> K <sup>-1</sup> )	log A' <sup>a</sup>	ΔS <sup>o</sup> <sup>b</sup> (J mol <sup>-1</sup> K <sup>-1</sup> )	ΔH <sup>o</sup> <sub>real</sub> (kJ mol <sup>-1</sup> )	ΔH <sup>o</sup> <sub>GC</sub> (kJ mol <sup>-1</sup> )	ΔH <sup>o</sup> <sub>ip</sub> (kJ mol <sup>-1</sup> )	ΔH <sup>o</sup> <sub>Z</sub> (kJ mol <sup>-1</sup> )	(ΔH <sup>o</sup> <sub>real</sub> ) <sub>corr</sub> (kJ mol <sup>-1</sup> )	ΔH <sup>o</sup> <sub>os</sub> <sup>c</sup> (kJ mol <sup>-1</sup> )	(ΔH <sup>o</sup> <sub>is</sub> ) <sub>exp</sub> (kJ mol <sup>-1</sup> )
Ru <sup>d</sup>	6(3)	3.4(4)	-7	23(2)	2	4	1	16	15	1
Fe <sup>d</sup>	11(3)	5.2(3)	9	32(2)	5	4	1	22	15	7
Fe <sup>e</sup>	31(3)	6.0(2)	35	36(1)	4	4	1	27	15	12
Ni <sup>d</sup>	18(3)	3.2(3)	-4	24(2)			1	23	15	8
Co <sup>e</sup>	95(23)	9.1(5)	137	57(3)	-9	-5	1	70	15	55

<sup>a</sup> A' = Ae<sup>ΔS<sup>o</sup>/R</sup> (eq 2), obtained from intercept of ln (k<sub>s,h</sub>)<sub>app</sub> versus 1/T. <sup>b</sup> From eq 12 using values of (k<sub>s,h</sub>)<sub>corr</sub> in Table 3 and A = 2 × 10<sup>3</sup> cm s<sup>-1</sup>. Rate constants obtained at Pt multiplied by 3 to account for difference in rate between the two electrode surfaces. <sup>c</sup> From eq 10 using ε<sub>s</sub> = 78.3, ε<sub>op</sub> = 1.78, ∂ε<sub>s</sub>/∂T = -0.36, ∂ε<sub>op</sub>/∂T = 0.00025, δ<sub>s</sub> = 82.6 pm, and r = 430 pm. <sup>d</sup> At Pt. <sup>e</sup> At Hg.

4. Figure 1 shows plots of the temperature dependence of the ln (k<sub>s,h</sub>)<sub>app</sub> for all four redox couples.

The parameter ΔH<sup>o</sup><sub>real</sub> is corrected by subtraction of three terms constituting enthalpic contributions to the electrochemical activation process<sup>19</sup>

$$(\Delta H_{\text{real}}^{\ddagger})_{\text{corr}} = \Delta H_{\text{real}}^{\ddagger} - (\Delta H_{\text{GC}}^{\ddagger} + \Delta H_{\text{ip}}^{\ddagger} + \Delta H_{\text{Z}}^{\ddagger}) \quad (9)$$

ΔH<sup>o</sup><sub>GC</sub> arises from the temperature dependence of the electrical double layer potential as estimated by Gouy–Chapman (GC) theory. ΔH<sup>o</sup><sub>ip</sub> describes the extent to which the temperature dependence of the bulk-solution ion-pair equilibrium (eq 5) influences the apparent kinetics, and ΔH<sup>o</sup><sub>Z</sub> represents the temperature dependence of the pre-exponential factor. ΔH<sup>o</sup><sub>GC</sub> is calculated from eqs 12 and 20–22 in ref 19 using Grahame's data for 0.7953 M NaF.<sup>38</sup> ΔH<sup>o</sup><sub>ip</sub> is calculated from the change in (k<sub>s,h</sub>)<sub>app</sub> produced by allowing ρ in eq 6 to assume a temperature dependence consistent with reaction 5 being endothermic to the extent of 6 kJ mol<sup>-1</sup>.<sup>39</sup> ΔH<sup>o</sup><sub>Z</sub> is equal to RT/2 = 1.25 kJ mol<sup>-1</sup>.

The experimental inner-shell enthalpy of activation is obtained from (ΔH<sup>o</sup><sub>real</sub>)<sub>corr</sub> by subtraction of the outer-shell enthalpy of activation calculated by the mean sphere approximation.<sup>40</sup>

$$\Delta H_{\text{os}}^{\ddagger} = \frac{-Ne^2}{8r} \times \left[ \left( 1 - \frac{1}{\epsilon_{\text{op}}} - \frac{T}{2\epsilon_{\text{op}}^2} \frac{\partial \epsilon_{\text{op}}}{\partial T} \right) - \left( 1 - \frac{1}{\epsilon_s} - \frac{T}{2\epsilon_s^2} \frac{\partial \epsilon_s}{\partial T} \right) \left( \frac{1}{1 + \frac{\delta_s}{r}} \right) \right] \quad (10)$$

$$(\Delta H_{\text{is}}^{\ddagger})_{\text{exp}} = (\Delta H_{\text{real}}^{\ddagger})_{\text{corr}} - \Delta H_{\text{os}}^{\ddagger} \quad (11)$$

In eq 10 r is the radius of the reactant, ε<sub>op</sub> and ε<sub>s</sub> are the optical and static dielectric constants of the solvent, and δ<sub>s</sub> is the solvent

polarization parameter. Values of (ΔH<sup>o</sup><sub>is</sub>)<sub>exp</sub> obtained from eq 11 are listed in the last column of Table 4.

The entropy of activation is calculated from eq 12,<sup>18b</sup> where

$$\Delta S^{\ddagger} = R \ln (k_{s,h})_{\text{corr}} + \frac{(\Delta H_{\text{real}}^{\ddagger})_{\text{corr}}}{T} - R \ln A \quad (12)$$

(k<sub>s,h</sub>)<sub>corr</sub> is the double-layer corrected rate constant at 25 °C (Table 3) and it is assumed that A = 2 × 10<sup>3</sup> cm s<sup>-1</sup>. Although this value is smaller than the quantity 5 × 10<sup>4</sup> cm s<sup>-1</sup> frequently employed in the encounter pre-equilibrium model of electrode kinetics,<sup>17</sup> it is chosen because it is consistent with experimentally observed prefactors for transition metal redox couples in aqueous solution.<sup>41</sup>

## Discussion

**Electrochemical Rate Constants.** Apparent values of the standard heterogeneous rate constants for M(tacn)<sub>2</sub><sup>3+</sup> reduction in Table 3 exhibit a dependence on NaF concentration that arises from a combination of electrical double layer and ion-pairing effects. The former of these terms dominates. Thus, in accordance with expectations for cationic reactants, the observed rate constants of couples which occur at potentials *negative* of the pzc<sup>42</sup> (Co) *increase* and those at potentials *positive* of the pzc (Fe, Ru) *decrease* with an increase in the absolute magnitude of φ<sub>2</sub>. The extent to which ion-paired forms participate in the electrode reaction is indicated qualitatively by the apparent transition state charge (z - α) obtained from Frumkin plots<sup>31</sup> of ln (k<sub>s,h</sub>)<sub>app</sub> versus φ<sub>2</sub> (not shown). This parameter should equal 2.5 for reduction of a tripositive cation when α = 0.5. Values of z - α = 2.3 are obtained for Co(tacn)<sub>2</sub><sup>3+</sup> reduction and 1.1–1.8 for the Ru(tacn)<sub>2</sub><sup>3+</sup> and Fe(tacn)<sub>2</sub><sup>3+</sup> reductions. This indicates that reduction proceeds primarily through non-ion-paired Co(tacn)<sub>2</sub><sup>3+</sup> and the 1:1 ion-paired forms of Fe(tacn)<sub>2</sub><sup>3+</sup> and Ru(tacn)<sub>2</sub><sup>3+</sup>.<sup>43</sup> The electrode kinetic data are corrected for the simultaneous influence of the electrical double-layer potential and ion-pair equilibrium by means of eq 6.

(38) Grahame, D. C. *J. Am. Chem. Soc.* **1957**, *79*, 2093. We thank Professor W. R. Fawcett for providing a copy of these data.

(39) This value is estimated from the enthalpy of ion-pair formation between Co(en)<sub>3</sub><sup>3+</sup> and halide ions: Evans, M. G.; Nancollas, G. H. *Trans. Faraday Soc.* **1953**, *49*, 363.

(40) Fawcett, W. R.; Blum, L. *Chem. Phys. Lett.* **1991**, *187*, 173.

(41) Hupp, J. T.; Liu, H. Y.; Farmer, J. K.; Gennett, T.; Weaver, M. J. *J. Electroanal. Chem.* **1984**, *168*, 313.

(42) The potential of zero charge of a mercury electrode in 0.2–1.0 M NaF is ca. -0.43 V vs SCE at 25 °C.<sup>30</sup>

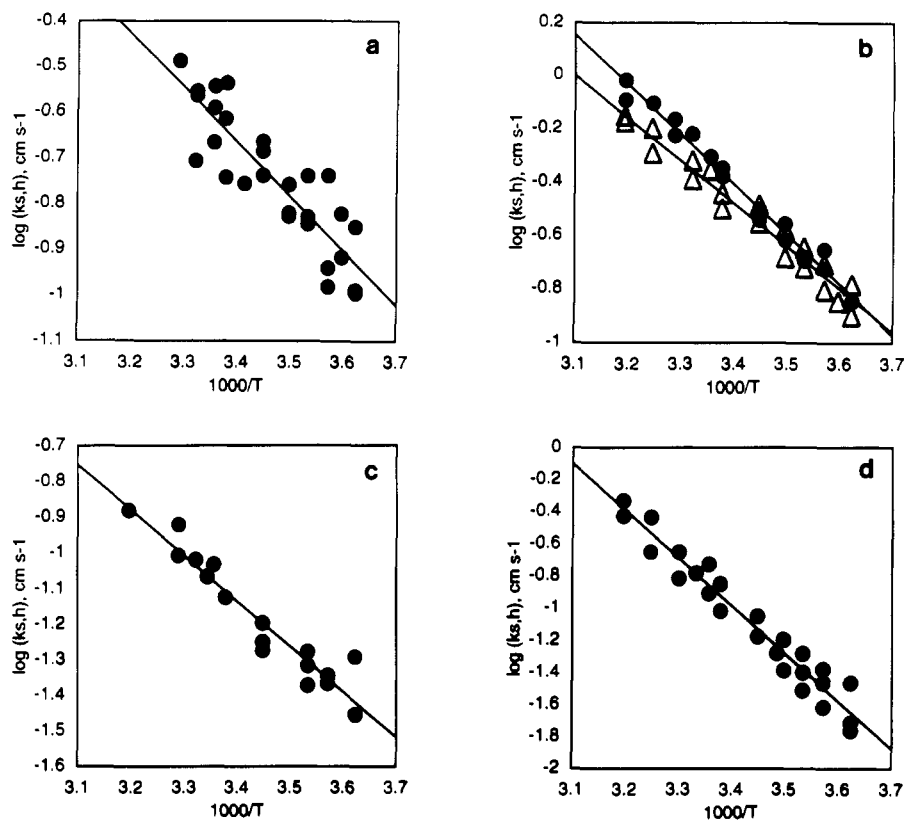


**Figure 1.** Plots of  $\log(k_{s,h})_{app}$  versus  $1/T$  for  $M(\text{tacn})_2^{3+/2+}$  redox couples in 0.75 M NaF: (a) Ru; (b) Fe ( $\bullet$  = Hg,  $\Delta$  = Pt); (c) Ni; (d) Co.

The corrected values of the standard heterogeneous rate constants are qualitatively in accord with results for other redox couples characterized by similar extents of structural change. For example, the result  $(k_{s,h})_{corr} = 1.3 \pm 0.2 \text{ cm s}^{-1}$  for  $\text{Ru}(\text{tacn})_2^{3+/2+}$  is close to that observed for  $\text{Ru}(\text{NH}_3)_6^{3+/2+}$  ( $2.0 \text{ cm s}^{-1}$  at Hg),<sup>44</sup> which by virtue of its similar size and small inner-shell barrier is anticipated to have a similar rate constant. The value of  $(k_{s,h})_{corr}$  obtained for  $\text{Co}(\text{tacn})_2^{3+/2+}$  is similar to that of  $\text{Co}(\text{en})_3^{3+/2+}$  ( $2.5 \times 10^{-2} \text{ cm s}^{-1}$ )<sup>41</sup> and therefore characteristic of  $\text{Co}(\text{III/II})$  couples which undergo large structural change in conjunction with electron transfer. Finally, the value of  $(k_{s,h})_{corr}$  determined for  $\text{Fe}(\text{tacn})_2^{3+/2+}$  at Pt is within a factor of 3 of the result at Hg, which is typical of rate constant ratios observed at these two electrode surfaces.<sup>45</sup> This result and the near coincidence of the  $\log(k_{s,h})_{app}$  versus  $1/T$  plots for  $\text{Fe}(\text{tacn})_2^{3+}$  reduction at Hg and Pt electrodes (Figure 1b) indicate that the electrode material does not exert a significant influence on the kinetic parameters.

The corrected standard heterogeneous rate constants at 25 °C decrease in the sequence  $\text{Ru} \sim \text{Fe} > \text{Ni} > \text{Co}$ . This order is qualitatively consistent with the extent of metal–ligand bond lengthening accompanying  $M(\text{tacn})_2^{3+}$  reduction and the kinetics of the corresponding homogeneous self-exchange reactions in Table 1. These relationships can be examined quantitatively in the following ways. First, if it is assumed that pre-exponential factors, outer-shell activation enthalpies and barrier-height corrections are identical for all half-reactions and that the inner-shell barrier of  $\text{Ru}(\text{tacn})_2^{3+/2+}$  is zero, division of each standard

heterogeneous rate constant by that of Ru provides an estimate of the inner-shell enthalpy of activation.

$$\Delta H_{is}^\ddagger = -RT \ln [k_{s,h}(M)/k_{s,h}(\text{Ru})] \quad (13)$$

By use of average  $(k_{s,h})_{corr}$  values obtained at Pt and division of the result for Co by 3 to account for the difference in rates between electrode surfaces, values of  $\Delta H_{is}^\ddagger = 1, 6,$  and  $14 \text{ kJ mol}^{-1}$  are calculated from eq 13 for Fe, Ni, and Co, respectively. These barrier heights are qualitatively consistent with the trend in electron-transfer reactivity but somewhat less than the calculated values of  $\Delta H_{is}^\ddagger$  in Table 1 and significantly smaller than the experimental ones in Table 4.

A second approach is to examine the correlation between heterogeneous and homogeneous rate constants predicted by Marcus–Hush theory<sup>1c</sup>

$$k_{s,h} = A_e(k_{ex})^{1/2}/A_h^{1/2} \quad (14)$$

where  $A_e$  and  $A_h$  are the pre-exponential factors for the electrochemical and homogeneous reactions, respectively. Figure 2 shows a plot of  $\log(k_{s,h})_{corr}$  versus  $\log(k_{ex})$  where the least squares slope of 0.44 is close to the coefficient 0.50 predicted by eq 14. In addition, close numerical correspondence between  $(k_{s,h})_{corr}$  and  $k_{ex}$  is achieved by use of values of  $A_e = 2 \times 10^3 \text{ cm s}^{-1}$  and  $A_h = 1 \times 10^{11} \text{ M}^{-1} \text{ s}^{-1}$ . Correlation between heterogeneous and homogeneous rate constants is anticipated.<sup>46</sup> The degree of agreement observed is high, although the number of points considered is small.

**Activation Parameters.** Metal-dependent effects on the kinetics and thermodynamics of reaction 1 are apparent in the activation parameters presented in Table 4. Significant aspects of these data are as follows: (i) experimental inner-shell

(43) The oxidized reactants are 50–83% ion-paired in bulk solution under the experimental conditions. At the OHP this fraction depends on the sign and magnitude of  $\phi_2$  and is calculated to be 5–67% in the case of  $\text{Co}(\text{tacn})_2^{3+}$  and 87–93% in the case of  $\text{Fe}(\text{tacn})_2^{3+}$  and  $\text{Ru}(\text{tacn})_2^{3+}$ .

(44) Gennett, T.; Weaver, M. J. *J. Anal. Chem.* **1984**, *56*, 1444.

(45) (a) Barr, S. W.; Guyer, K. L.; Weaver, M. J. *J. Electroanal. Chem.* **1980**, *111*, 41. (b) Iwasita, T.; Schmickler, W.; Schulze, J. W. *Ber. Bunsen-Ges. Phys. Chem.* **1985**, *89*, 138.

(46) (a) Hupp, J. T.; Weaver, M. J. *J. Phys. Chem.* **1985**, *89*, 2795. (b) Weaver, M. J. *J. Phys. Chem.* **1990**, *94*, 8608.

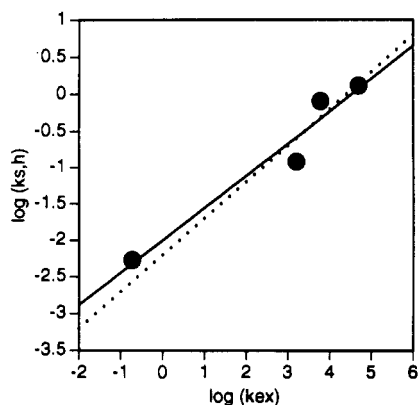


**Figure 2.** Plot of  $\log(k_{s,h})_{\text{corr}}$  versus  $\log(k_{\text{ex}})$  for  $\text{M}(\text{tacn})_2^{3+/2+}$  redox couples. The solid line is a linear least-squares regression of the data. The dotted line is the correlation predicted by eq 14.

enthalpies of activation,  $(\Delta H_{\text{is}}^{\ddagger})_{\text{exp}}$ , encompass a large range of values which exhibits a sequence ( $\text{Co} \gg \text{Fe} \sim \text{Ni} > \text{Ru}$ ) in qualitative accord with the redox induced changes in  $\text{M}-\text{N}$  bond distances, albeit values for Fe and Co are larger than calculated via eq 4; (ii) significant nonzero and metal-dependent values are obtained for  $\Delta S_{\text{rc}}^{\circ}$  and  $\Delta S^{\ddagger}$ ; (iii) there is close correlation between these entropic terms and  $(\Delta H_{\text{is}}^{\ddagger})_{\text{exp}}$  as illustrated in Figure 3. The following paragraphs discuss these points.

Inner-shell contributions to the enthalpy of activation are obtained by correction of experimentally determined barrier heights by eqs 9–11. Two observations support the accuracy of this procedure. (1) The magnitudes of the double layer and ion-pairing corrections are small and (with the exception of Co) approximately equal for all reactants. This condition is realized by use of a large concentration of sodium fluoride electrolyte, which minimizes the correction for the temperature dependence of the double layer potential while introducing only a small contribution from ion-pairing. (2) A negligible inner-shell barrier is obtained for  $\text{Ru}(\text{tacn})_2^{3+/2+}$ , consistent with the small change in  $\text{M}-\text{N}$  bond distance for this couple. This is achieved by use of a value of  $\Delta H_{\text{os}}^{\ddagger} = 15 \text{ kJ mol}^{-1}$  calculated via the mean spherical approximation,<sup>40</sup> which provides a result ca. 7  $\text{kJ mol}^{-1}$  smaller than conventional dielectric continuum theory (eq 10 lacking the term in  $\delta_j/r$ ). The mean spherical approximation has been suggested to be a more accurate method of calculating outer-shell reorganization energies,<sup>4c</sup> and the result  $(\Delta H_{\text{is}}^{\ddagger})_{\text{exp}} \sim 0 \text{ kJ mol}^{-1}$  obtained for  $\text{Ru}(\text{tacn})_2^{3+/2+}$  supports this view.

$(\Delta H_{\text{is}}^{\ddagger})_{\text{exp}}$  is the inner-shell component of the real enthalpy of activation and is the experimental parameter most closely related to inner-shell part of the Marcus reorganization energy.<sup>18a</sup> Anticipated values of  $(\Delta H_{\text{is}}^{\ddagger})_{\text{exp}}$  are obtained for Ru and Ni. However, significant differences exist between  $(\Delta H_{\text{is}}^{\ddagger})_{\text{exp}}$  and  $(\Delta H_{\text{is}}^{\ddagger})_{\text{calc}}$  for  $\text{Fe}(\text{tacn})_2^{3+/2+}$  and  $\text{Co}(\text{tacn})_2^{3+/2+}$ . These couples also exhibit the largest values of  $\Delta S_{\text{rc}}^{\circ}$  and  $\Delta S^{\ddagger}$ .

We have considered several possible reasons for the observed discrepancies in these inner-shell activation enthalpies. First, the calculated values of  $\Delta H_{\text{is}}^{\ddagger}$  are influenced by the accuracy of the X-ray structural data. If an uncertainty of  $\pm 2\sigma$  is assigned to the  $\text{M}-\text{N}$  bond distances in Table 1, then  $(\Delta H_{\text{is}}^{\ddagger})_{\text{calc}} = 0 \pm 1, 1 \pm 3, 9 \pm 5, \text{ and } 25 \pm 21 \text{ kJ mol}^{-1}$  for Ru, Fe, Ni, and Co, respectively. These ranges provide better agreement with experimental results, but are not large enough to account for the anomalous observations for Fe and Co. Second, a single reduced force constant of  $f_i = 170 \text{ N m}^{-1}$  is used in the calculation of barrier heights. However, since metal–amine stretching frequencies are not highly dependent on the identity

of M for first row transition elements,<sup>47</sup> a greatly incorrect estimate of  $\Delta H_{\text{is}}^{\ddagger}$  is not likely to arise from this source. Even so, changes in all internal degrees of freedom rather than just  $\text{M}-\text{N}$  bond distances should be considered in interpreting observed differences in  $\Delta H_{\text{is}}^{\ddagger}$  for these complexes, and studies to address this issue employing quantum and molecular mechanics are underway and will be reported at a later date.<sup>48</sup> Finally, we consider the possibility that temperature-dependent contributions to ion-pairing and electrical double layer effects beyond those included in eq 9 account for some of the differences in  $(\Delta H_{\text{is}}^{\ddagger})_{\text{exp}}$ .<sup>49</sup> However, it is difficult to imagine that such factors could result in the observed metal dependences and deviations in the same direction for reactants (Fe and Co) whose redox potentials occur on opposite sides of the potential of zero charge. Thus, we conclude that the observed values of  $(\Delta H_{\text{is}}^{\ddagger})_{\text{exp}}$  represent a real manifestation of  $\text{M}(\text{tacn})_2^{3+/2+}$  electron-transfer behavior.

We next inquire into the magnitudes of  $\Delta S_{\text{rc}}^{\circ}$  and  $\Delta S^{\ddagger}$  and their correlations with  $(\Delta H_{\text{is}}^{\ddagger})_{\text{exp}}$  (Figure 3). Both entropic parameters exhibit significantly metal-dependent values. Furthermore, the values of  $\Delta S^{\ddagger}$  are consistent with the intercepts of the experimental  $\log(k_{s,h})_{\text{app}}$  versus  $1/T$  plots ( $\log A'$  in Table 4), whose magnitudes ( $A' \geq 2 \times 10^3 \text{ cm s}^{-1}$ ) argue against significant involvement of nonadiabaticity ( $\kappa_{\text{el}} < 1$ ) or nuclear tunneling ( $\Gamma_{\text{n}}$ ) in the electrode reactions.

Half-reaction entropies have been measured for transition metal redox couples on many occasions.<sup>24,50</sup> The parameter commonly is described in terms of a Born solvation model, wherein the size and charge of the product and reactant are the primary determinants of  $\Delta S_{\text{rc}}^{\circ}$  with contributions arising also from the ligands and ligand–solvent interactions. However, these factors are invariant for reaction 1, which suggests that the metal-dependent differences in  $\Delta S_{\text{rc}}^{\circ}$  and  $\Delta S^{\ddagger}$  derive from other sources. The  $\sim 90 \text{ J mol}^{-1} \text{ K}^{-1}$  difference in  $\Delta S_{\text{rc}}^{\circ}$  between  $\text{Co}(\text{tacn})_2^{3+/2+}$  and  $\text{Ru}(\text{tacn})_2^{3+/2+}$  is typical of that observed between isostructural  $\text{Co}(\text{III/II})$  and  $\text{Ru}(\text{III/II})$  couples. Richardson and Sharpe<sup>51</sup> recently proposed that a large part of this difference arises from inner-shell contributions to the vibrational entropy of the reaction. The contribution is expressed in terms of the vibrational partition functions of the oxidized and reduced species and differs significantly from zero when vibrational frequencies are low and change substantially upon a change in oxidation state. The later conditions characterize the metal–ligand skeletal vibrations of many transition metal complexes, particularly those which experience a change in the number of bonding or antibonding electrons upon redox. This phenomenon, operating to varying extents, is proposed as an explanation for the metal-dependent values of  $\Delta S_{\text{rc}}^{\circ}$  in Table 4.

A parallel range of metal-dependent values is observed for  $\Delta S^{\ddagger}$ . The magnitude of this parameter for Fe and Co is surprising, because the intrinsic entropy of activation of electrode reactions is considered to be small.<sup>17</sup> However, this conclusion pertains to systems which can be defined in terms of a single

(47) Schmidt, K. H.; Müller, A. *Inorg. Chem.* **1975**, *14*, 2183.

(48) Gao, Y.-D.; Lipkowitz, K. B.; Schultz, F. A. Work in progress.

(49) Examination of this possibility requires obtaining temperature-dependent rate data in electrolytes whose ion-pairing and double layer properties are well-established and different from those of NaF. Studies of this type are planned.

(50) (a) Yee, E. L.; Weaver, M. J. *Inorg. Chem.* **1980**, *19*, 1077. (b) Sahami, S.; Weaver, M. J. *J. Electroanal. Chem.* **1981**, *122*, 155. (c) Sahami, S.; Weaver, M. J. *J. Electroanal. Chem.* **1981**, *122*, 171. (d) Hupp, J. T.; Weaver, M. J. *Inorg. Chem.* **1984**, *23*, 3639. (e) Hupp, J. T.; Weaver, M. J. *J. Phys. Chem.* **1984**, *88*, 1860.

(51) (a) Richardson, D. E.; Sharpe, P. *Inorg. Chem.* **1991**, *30*, 1412. (b) Richardson, D. E.; Sharpe, P. *Inorg. Chem.* **1993**, *32*, 1809.

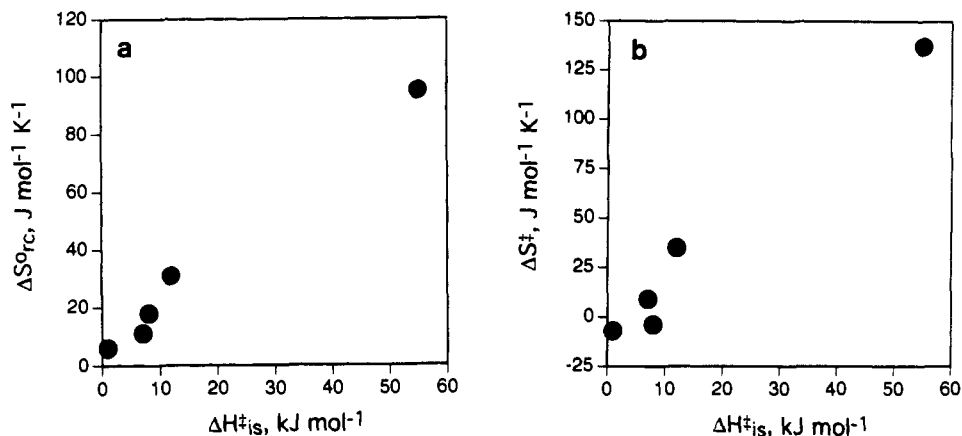


**Figure 3.** Plots of (a)  $\Delta S^{\circ}_{rc}$  and (b)  $\Delta S^{\ddagger}$  versus  $(\Delta H^{\ddagger}_{is})_{exp}$  for  $M(tacn)_2^{3+/2+}$  redox couples in 0.75 M NaF.

force constant for reduced and oxidized species. When large differences exist in vibrational frequency between reactant and product species, large entropy differences can result and lead to unusual consequences in the activation of electron-transfer reactions.<sup>52</sup> Whereas application of this principle appears straightforward in rationalizing observed  $\Delta S^{\circ}_{rc}$  values in terms of vibrational partition functions,<sup>51</sup> we are less well prepared to say how it is manifest in electrochemical entropies of activation. However, the correlation among  $\Delta S^{\ddagger}$ ,  $\Delta S^{\circ}_{rc}$ , and  $(\Delta H^{\ddagger}_{is})_{exp}$  and the compensation of entropic and enthalpic terms in the electrochemical rate expression (eq 2) suggest that these observations derive from a single (or at least related) explanation for  $M(tacn)_2^{3+/2+}$  reactions.

Because structural change accompanying a change in oxidation state does not occur infrequently in transition metal redox chemistry, it is of interest to inquire if similar effects are observable under other circumstances. Weaver and Sutin<sup>53</sup> reported a correlation between the reorganization energies and half-reaction entropies for a series of homogeneous electron-transfer reactions characterized by large structural change. The result was attributed to entropic differences in solvent polariza-

tion arising from the difference in size of the oxidized and reduced reactants. However, for homologous series of compounds (e.g., aquo metal ion redox couples) examined in their study, partial explanation in terms of inner-shell vibrational effects operating both in  $\Delta H^{\ddagger}_{is}$  and  $\Delta S^{\circ}_{rc}$  is consistent with the conclusions presented here. A second example is found in a recent study of gas phase electron attachment to ( $\eta^4$ -olefin)-iron tricarbonyls.<sup>54</sup> Loosening of the iron-olefin bond upon electron addition results in creation of large inner-shell barriers, attenuation of gas-phase electron-transfer kinetics, and appearance of significant half-reaction entropies. The effects are less apparent in analogous Cr compounds, which exhibit a smaller degree of metal-olefin bond weakening. On the basis of these observations, inner-shell effects may be more prevalent in electron transfer kinetics than previously anticipated and further characterization of their role in these reactions is desirable.

**Acknowledgment.** Support of this research by the National Science Foundation (Grant CHE-9214748) is gratefully acknowledged. We thank Professors Mike Weaver and Ron Fawcett for helpful discussions and Professor Fawcett for providing the temperature-dependent double layer data of D. C. Grahame and a copy of ref 4c prior to publication. We also thank an anonymous reviewer for pointing out a conceptual error in an earlier version of this manuscript.

(52) (a) Marcus, R. A.; Sutin, N. *Inorg. Chem.* **1975**, *14*, 213. (b) Hupp, J. T.; Weaver, M. J. *J. Phys. Chem.* **1984**, *88*, 6128. (c) Hupp, J. T.; Neyhart, G. A.; Meyer, T. J.; Kober, E. M. *J. Phys. Chem.* **1992**, *96*, 10820. (d) Weintraub, O.; Bixon, M. *J. Phys. Chem.* **1994**, *98*, 3407.  
 (53) Sutin, N.; Weaver, M. J.; Yee, Y. L. *Inorg. Chem.* **1980**, *19*, 1096.

(54) Sharpe, P.; Kebarle, P. *J. Am. Chem. Soc.* **1993**, *115*, 782.